Contents lists available at ScienceDirect

Catena

Characterization of granitoid and gneissic weathering profiles of the Mucone River basin (Calabria, southern Italy)

L. Borrelli [a], F. Perri [b,*], S. Critelli [b], G. Gullà [a]

[a] CNR-IRPI_U.O.S. di Cosenza, Via Cavour n. 4/6, 87036 Rende (CS), Italy
[b] Università degli Studi della Calabria, Dip. di Biologia, Ecologia e Scienze della Terra, 87036 Rende (CS), Italy

ARTICLE INFO

ABSTRACT

The paper deals with the development of a multidisciplinary research on weathering profiles of granitoid and gneissic rocks related to tectonic and landscape evolution of the western Sila Grande Massif (Calabria, southern Italy). Field scale observations and petrographical and mineralogical features are used to characterize in detail the weathering processes. The weathering profiles of the granitoid cut slopes are generally simple showing a progressive weathering increase toward the top of the slopes, whereas the weathering profiles of the gneissic cut slopes are generally complex with irregularities in the spatial distribution of weathered horizons. The microfabric and petrographic analyses show that gneissic samples (classes V–VI of weathering grade) are characterized by higher percentage of altered minerals and microfracture and void rather than granitoid samples (classes V–VI of weathering grade). The main mineralogical changes concern the partial transformation of biotite and the partial destruction of feldspars (mainly plagioclases), associated with the neoformation of secondary minerals (clay minerals and Fe-oxides) and with a substitution of the original rock fabric. Neoformed clay minerals and ferruginous products replaced feldspars and biotite during the most advanced weathering stage. Referred as physical changes coupled with chemical variations, the final results of weathering process are a soil-like material characterized by sand–gravel grain-size fraction for the granitoid rocks and by both silt–clay and sand–silt grain-size fraction for the gneissic rocks. This generally produces a greater value of the SGI (Sand Generation Index) for granitoids and explains the great productivity in sandy deposits of this lithology.

1. Introduction

Weathering process is one of the most important phenomena affecting the dynamic equilibrium of earth's crust. Chemical and physical transformations of several types of rocks (metamorphic, magmatic, and sedimentary) are related to weathering processes occurred under a variety of climatic conditions all over the world. These changes affect almost all the engineering properties of rocks and in most cases these effects are unfavorable as they reduce both strength and then stability of rock masses. These latter, in turn, may produce adverse geomorphological effects, such as bed incision driven by the increased sediment transport capacity and the lack of sediment replacement from upstream. The geomorphological effects of weathering range from esthetic change to landscape evolution (e.g., Ollier, 1983, 1984, 1988; Whalley and Turkington, 2001).

Weathering of crystalline rocks (plutonic and metamorphic), related to physical disintegration and chemical decomposition, affects both rock materials and rock masses. Physical weathering breaks down rock masses along their crystal boundaries; chemical weathering (e.g., hydrolysis, oxidation, dissolution) preferentially alters feldspars and biotite minerals, leaving behind a residue of quartz and other weathering resistant minerals. Furthermore, weathering produces mineralogical and petrographical transformations and, thus, a considerable decay of the physical–mechanical properties of the original rock (Baynes and Dearman, 1978a,b; Irfan and Dearman, 1978), predisposing the weathered crystalline rocks to mass movement phenomena (e.g., Borrelli, 2008; Borrelli et al., 2007, 2012; Brand and Phillipson, 1985; Calcaterra et al., 1998; Cascini and Gullà, 1993; Cascini et al., 1992, 1994; Critelli et al., 1991; Deere and Patton, 1971; Gullà et al., 2004). Commonly, slope instabilities are related to the features of weathering profiles (Borrelli, 2008; Ruxton, 1958). Weathering profile is a vertical assemblage of different weathering zones from the surface soil to the unaltered bedrock. The term "soil" is here used to indicate deposits of residual and colluvial nature, without any relations to 'pedogenetical processes' (G.S.E.G.W.P., 1995). The characterization of weathering profiles is generally used by geotechnical and engineering geological researchers (Baynes et al., 1978; G.S.E.G.W.P., 1995; Ruxton, 1958) to evaluate the predisposition factors relative to different landslide typologies.

This work represents an integrated analysis of the weathering processes occurred on the granitoid and gneissic rock profiles, along the north-western slopes of the Sila Massif (northern Calabria, Italy); the studied area is located on the central sector of the Mucone River basin. Diffuse landslides with occasional deep-seated gravitational

* Corresponding author. Tel.: +39 0984493550.
E-mail address: francesco.perri@unical.it (F. Perri).

slope deformations have been long recognized in the studied area (Borrelli, 2008; Borrelli et al., 2007; Garfì et al., 2007; Gullà et al., 2004; Sorriso-Valvo and Tansi, 1996; Terranova et al., 2007).

In this work the weathering profiles for granitoid and gneissic rocks have been described and characterized based on field studies and minero-petrographical and chemical analyses. In the field, the granitoid and gneissic rocks were described in terms of their weathering grade defined on the basis of visual descriptions and a number of simple index tests (e.g., discoloration, samples broken by hands and hammer, Schmidt Hammer tests). Extensive surface and subsurface investigations were used to determine the characteristics and depth of weathering profiles developed in the rocks. The field descriptions and the weathering characterizations were verified by means of minero-petrographical and chemical analyses. Thus, the physical, chemical and minero-petrographical changes at each grade of weathering have been determined.

2. The Sila Massif

The Sila Massif (Fig. 1) is mainly characterized by metamorphic and granitoid Alpine and Hercynian rocks covered in places by unmetamorphosed Mesozoic sedimentary rocks (the Longobucco Group), and it represents a section of the Hercynian orogenic belt of
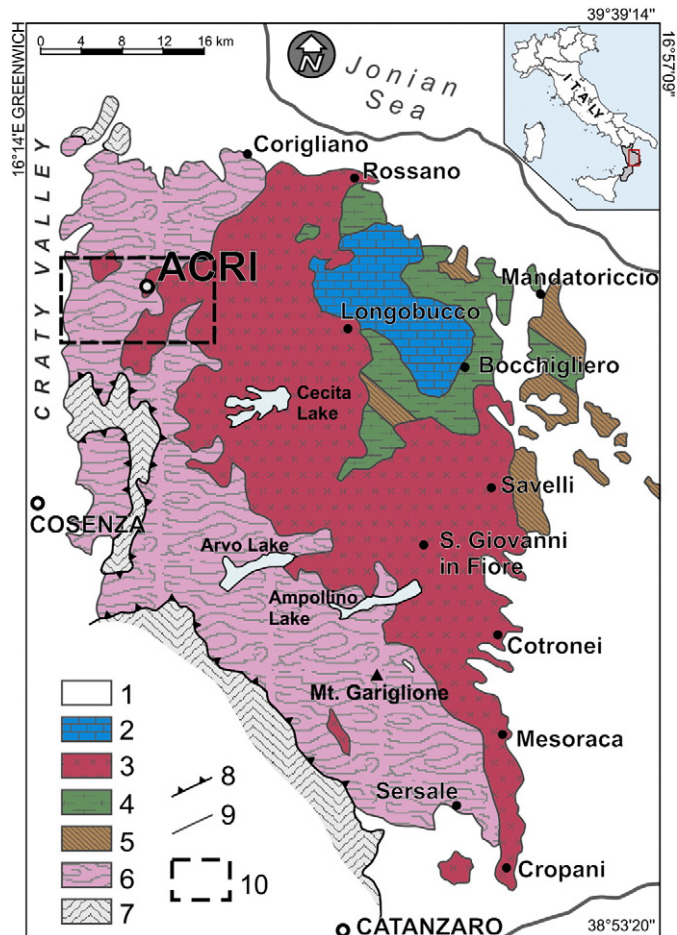

Fig. 1. Geologic sketch of the Sila Massif with location of the study area. Legend: 1) predominantly clastic deposits (Recent to Tortonian). 2 to 6 = Sila Unit: 2) Mesozoic to Tertiary sedimentary cover; 3) plutonic rocks (Sila Batholith; Carboniferous–Permian); 4) low-grade metamorphic rocks (Bocchiglero Complex; Late Cambrian to Early Carboniferous); 5) low- to medium-grade metamorphic rocks (Mandatoriccio Complex; Late Cambrian to Early Carboniferous); 6) medium- to high-grade metamorphic rocks (Monte Gariglione–Polia–Copanello Complex; pre-Triassic); 7) Lower Alpine thrust nappes of the Sila Massif including Castagna, Bagni and Ophhiolitic Units (phyllite + schist and ophiolitic rocks); 8) thrust fault; 9) stratigraphic contact; 10) studied area. Modified from Messina et al. (1991).

western Europe (e.g., Bonardi et al., 2001). The Paleozoic metamorphic rocks mainly consist of gneiss, schist and phyllite, affected by various Alpine metamorphic events and intruded by the Late Hercynian Sila Batholith (Messina et al., 1991, 1994). The Paleozoic intrusive rocks (Sila Batholith) are composed by granitoids with a composition ranging from granodiorite to gabbro and leucomonzogranite (Messina et al., 1991). The exhumation history of the Sila Massif, based on the apatite fission track (AFT) analyses, is characterized by rapid cooling of the crystalline basement rocks between 35 My and 15 My as a result of crustal extension and subaerial erosion (Thomson, 1994).

The regional tectonic evolution shows that the Sila Massif structural high had already emerged during the middle Miocene (e.g., Corbi et al., 2009; Matano and Di Nocera, 1999; Tripodi et al., 2013). The development of weathering profiles in Sila could have occurred between the late Miocene and the Pleistocene under various climatic conditions (e.g., Critelli et al., 1991; Guzzetta, 1974; Ietto and Ietto, 2004; Matano and Di Nocera, 1999; Mongelli et al., 1998). Under the current temperate and Pleistocene glacial climatic conditions, the erosional processes, as activated by tectonic uplifting, prevail over weathering processes, although not enough to completely remove the exposed, deeply weathered mantle (e.g., Calcaterra and Parise, 2010; Ietto and Ietto, 2004; Le Pera and Sorriso-Valvo, 2000a,b; Matano and Di Nocera, 1999).

## 3. Morphological and geological features of the Mucone River basin

The study area is located in the west-central side of the Mucone River basin, on the north-western slope of the Sila Massif (northern Calabria) (Fig. 2). The area extends about 100 km² and ranges in elevation from 200 to 1100 m a.s.l.; the climate is Mediterranean-type (Cs, sensu Köppen, 1936), with summer as dry season and precipitation concentrated in mild winters. The drainage network is mainly controlled by the discontinuities produced by Quaternary tectonics. The drainage system is dense and often cuts the bedrock (e.g., Cascini et al., 1992).

The investigated area shows evidence of glacial events, probably belonging to the last glacial age (Late Würm), between 21 and 18 ka (Palmentola et al., 1990), which contributed to shape its main morphologies. Three main morphological sectors can be distinguished: the highplains, the slopes, and the valley. Highplains are the highest and represent the remnants of an ancient morphological surface partially removed by erosion (e.g., Molin et al., 2004; Olivetti et al., 2012; Scarciglia et al., 2005). They are morphodynamically inactive, even if slow rock alteration occurs in situ, under-present climatic conditions. The slopes are characterized by high gradient values (about 30°–40°) and deep incisions up to crystalline basement, where erosion and mass movements are widespread because the very active morphodynamics of the slopes. The valley is mostly characterized by sedimentation (e.g., detrital deposition systems such as alluvial debris flow fan and detrital fan), with local erosional processes.

The Palaeozoic crystalline lithologies, outcropping in the study area (Fig. 2), are mainly represented by the Sila Unit (Messina et al., 1994), including medium- to high-grade metamorphic and granitoid rocks.

The gneissic rocks are composed by high-grade metamorphic rocks, represented by medium- to coarse-grained biotite-garnet and sillimanite gneiss, outcropping along the Mucone River, and medium- to coarse-grained biotite–muscovite migmatitic gneiss, outcropping close to the contact with the granitoid rocks (Fig. 2). These rocks are dark, reddish to purple in color, from schistose to massive. The biotite–garnet–sillimanite-rich gneissic rocks are mainly characterized by quartz–feldspar-rich layers having coarse-grained garnets, interbedded with biotite–sillimanite dark layers. Leucosomathic portions of gneiss are thick few decimeters.

The granitoid rocks mainly outcrop in the eastern part of the studied area (Fig. 2). They are mainly composed of tonalite, passing locally to granodiorite, and minor granodiorite with K-feldspar phenocrysts. The predominant constituent minerals are also represented of plagioclase, quartz, biotite and muscovite. These rocks are coarse-grained, white
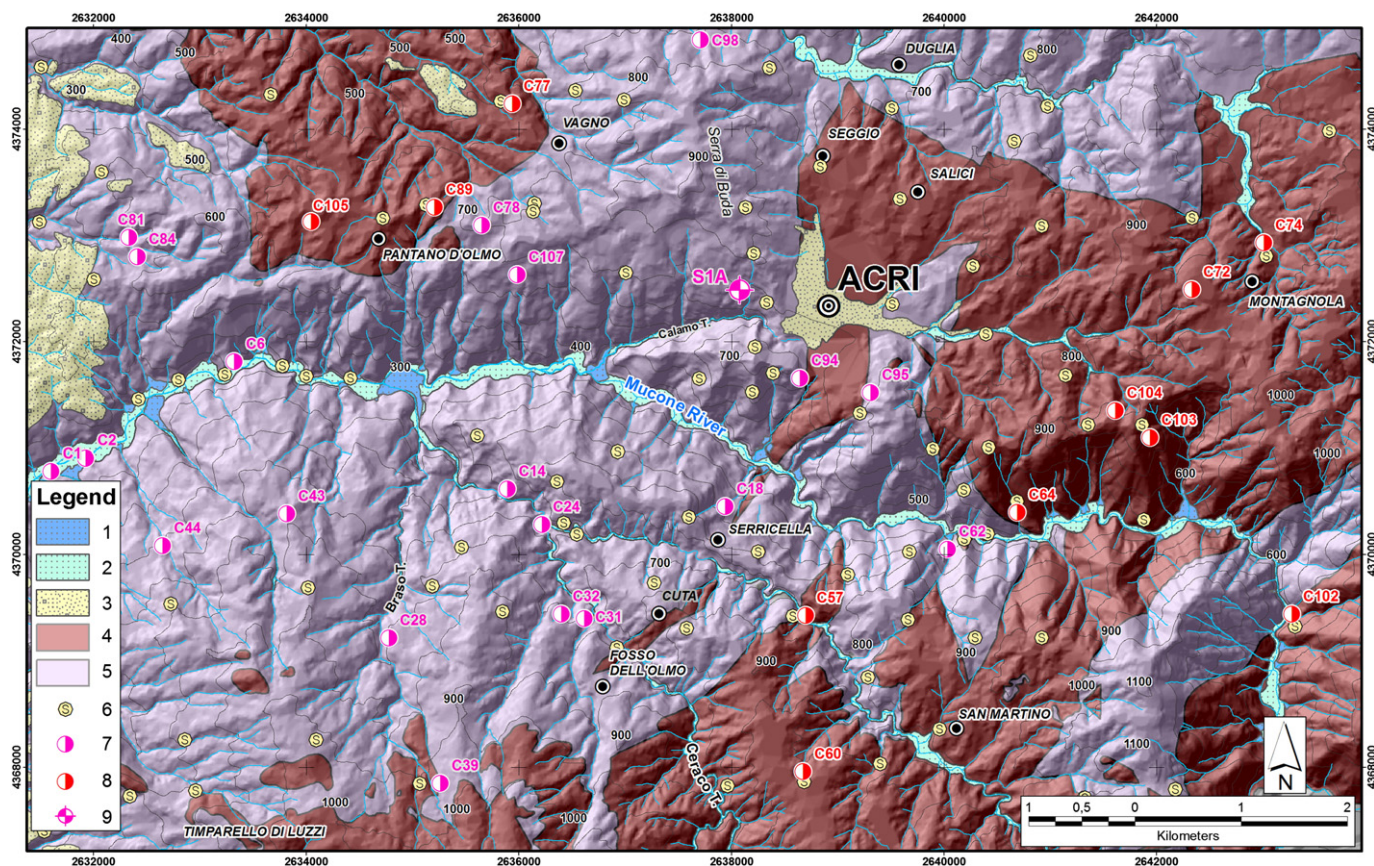
Fig. 2. Simplified geological map of the western-central side of the Mucone River Basin (northern Calabria, Italy). Legend: 1) alluvial and debris fan (Holocene); 2) alluvial deposits (Holocene); 3) matrix-supported conglomerates (Lower–Middle Pleistocene); 4) granitoid rocks (Paleozoic); 5) gneissic rocks (Paleozoic); 6) studied weathering profiles; 7) samples from cut slope weathering profiles of gneissic rocks; 8) samples from cut slope weathering profiles of granitoid rocks; 9) samples from borehole (S1A).

and pink in color. Generally the granitoid rocks are intruded by pegmatite and aplite dikes. The granitoid and gneissic rocks, often covered with thickness of colluvial deposits, are intensely weathered. Generally, the contact between granitoid and gneiss is tectonic.

Landslide and deep-seated gravitational slope deformations are found along the borders of the Mucone River (Borrelli et al., 2007, 2011a,b; Sorriso-Valvo and Tansi, 1996; Terranova et al., 2007), where local relief energy and steep slopes are commonly associated with severe tectonic fracturing. In particular, in the study area have been identified and mapped from Borrelli et al. (2007) three types of landslide: debris flow, debris slide and rock slides.

4. Methods

In order to have more data on the thickness and geometrical characteristics of the different weathering horizons, a detailed survey of weathering profiles has been performed based on evaluation of 70 cut slopes (Fig. 2). The elevation of the cut slopes range from 210 m to 1100 m a.s.l. The Mucone River is characterized by deep incision with steep slopes where bedrock crops out. These morphological features allow us to define the typical weathering profile for the granitoid and gneissic rocks.

The weathering profiles have been studied following the methodology proposed by Gullà and Matano (1997). Both qualitative (e.g., rock color, discoloration processes, samples broken by hands and hammer) and quantitative (e.g., Schmidt Hammer tests) criteria were used to classify the observed weathering grades on each cut slope.

Samples were collected along granitoid and gneissic weathering profiles during the field survey (35 samples), which provides a continuous

record from fresh plutonic and metamorphic rocks to residual soils (Fig. 2).

Samples collected for each weathering class, were thin sectioned for microfabric and petrographic analysis. In particular, the completely weathered rocks and residual soils were cemented with epoxy resin and successively thin sectioned. The weathering progress has been characterized using petrographics indices for quantifying the changes in the intrinsic properties of rocks from different points of view, some of which can be related to the engineering properties of weathered rocks. The most commonly used are the decomposition index (X_d; Lumb, 1962), indicating the extent to which the rock microfabric and composition are affected by weathering, and the micropetrographic index (I_p; Irfan and Dearman, 1978), defined as a ratio among primary and accessory unaltered minerals and secondary minerals together with microcracks and voids. The studied samples have been also investigated by scanning electron microscope (SEM) on the fractured surfaces; EDS (energy dispersive X-ray spectroscopy) analyses were performed on a FEI Quanta 200 scanning electron microscope equipped with EDAX Genesis 4000, at the Università della Calabria (Italy).

The mineralogy of the whole rock and the fine fraction (<2 μm) were determined by X-ray powder diffraction (XRD; Bruker D8 Advance diffractometer, with CuKα radiation in the range 5°–60° 2θ, with steps of 0.02° 2θ and step-times of 1 s/step) at the Università della Calabria (Italy). The fine fraction (clay suspension) was separated by centrifugation; successively the oriented mounts prepared from clay suspensions, were air-dried, glycolated at 60 °C overnight, and heated at 375 °C for 1 h. X-ray diffraction analyses were carried out according to Moore and Reynolds (1997). The occurrence of clay minerals in the <2 μm grain-size fraction was estimated on both glycolated and heated oriented mounts (e.g., Perri, 2008; Perri et al., 2011b).

Table 1
Descriptions assumed as reference for the weathering classes.
Modified from Gullà and Matano (1997).

Class	Rock mass	Rock material
I — Fresh	The rock mass is fresh (more than 70% of the outcrop); limited and isolated rock mass volumes, near the discontinuities, can be constituted by slightly weathered rock.	Rock unchanged from original state or only slightly stained along major joints.
II — Slightly weathered	The rock mass is slightly weathered (more than 70% of the outcrop); limited and isolated rock mass volumes, near the discontinuities, can be constituted by moderately weathered rock.	The rock material has mainly the following characteristics: same color of the fresh rock (class I) with discoloration only near the discontinuities; original texture and microstructure of the fresh rock are perfectly preserved; strength is comparable to that of the fresh rock (hard rock); make a ringing sound when it is struck by hammer. $N_{Schmidt}$ value more than 50.
III — Moderately weathered	The rock mass is moderately weathered (more than 70% of the outcrop); limited and isolated rock mass volumes can be constituted by highly or slightly weathered rock.	The rock material has mainly the following characteristics: pervasively discolored, but locally the color of the fresh rock can be present; original texture and microstructure of the fresh rock are well preserved; strength is comparable to that of the fresh rock (hard rock); make an intermediate sound when it is struck by hammer; large pieces are hardly broken if they are struck by head of hammer; point of geological hammer can produce a scratch on the surface of rock. $N_{Schmidt}$ value: 25–50.
IV — Highly weathered	The rock mass is highly weathered (more than 70% of the outcrop); limited and isolated rock mass volumes can be constituted by moderately or completely weathered rock. The volumes constituted of residual soils, rarely in outcrop and usually located on crowns, present the sand and silts fractions prevalent.	The rock material has mainly the following characteristics: completely discolored; original texture and microstructure of the fresh rock are still preserved; strength is substantially reduced (weak rock); make an intermediate dull sound when it is struck by hammer; large pieces are easily broken if they are struck by hammer; large pieces do not slake in water; point of geological hammer indents the rock superficially; knife edge produces a scratch on the surface of rock. $N_{Schmidt}$ value: 10–25.
V — Completely weathered	The rock mass is completely weathered (saprolite) (more than 70% of the outcrop); limited and isolated rock mass volumes can be constituted by completely weathered rock or residual soil. The volumes constituted of completely weathered rock, usually are located at the upper reaches of the slopes (generally above 700 m above sea level).	The rock material has mainly the following characteristics: completely discolored; original texture and microstructure of the fresh rock are present in relict form; soil like behavior; large pieces can be broken by hand and slake in water; point of geological pick indents the rock deeply; knife edge easily carves the surface of rock; gravel and sand fractions are prevalent. $N_{Schmidt}$ value: 0–15.
VI — Residual and colluvial soil	The rock mass mainly consists of residual, colluvial and detrital–colluvial soils (more than 70% of the outcrop); limited and isolated portions can be constituted by moderately or highly weathered rock and/or saprolitic soil.	The rock material has mainly the following characteristics: completely discolored; original texture and microstructure of the fresh rock are completely destroyed; soil like behavior; large pieces can be easily broken by hand and crumbled by finger pressure into constituent grains. The volumes constituted of residual soils, rarely in outcrop and usually located on crowns, present the sand and silts fractions prevalent. The volumes constituted of colluvial soils, usually located on slope and into morphological hollows, are formed by sandy–silty chaotic deposits, including moderately to highly weathered centimetric rock fragments and subordinately organic fragments. The volumes constituted of detrital–colluvial soils, located on the lower portions of slopes, are represented by disorganized structure deposits, formed by sand and gravel including moderately to highly weathered decimetric rock fragments and subordinately organic fragments.

5. Results

5.1. Survey of weathering profiles

Five classes of weathering have been recognized in the studied area: from the class VI (residual and colluvial soils) to the class II (slightly weathered rock). Limited volumes of class I (fresh rock) have been locally found within the class II. The characteristics of the different weathering classes for granitoid and gneiss rocks are summarized in Table 1.

The weathering profiles observed on the granitoid cut slopes (Fig. 3) are generally simple (sensu Brand and Phillipson, 1985) and characterized by a progressive weathering increase toward the top of the slopes. Generally, the weathering profiles are characterized by rocky masses varying from slightly weathered rocks (along the cut slopes of the stream incisions) to completely weathered rocks (along cut slopes of the highest reliefs). Corestones are not common in the studied granitoid cut slopes. Residual soils (class VI) are locally observed in the highest reliefs (Fig. 2) and are few centimeters thick. Faults and fractured zones are commonly present on the cut slopes examined, where sharp contacts between the different weathering classes are observed (Fig. 3). The most important discontinuities are characterized by completely weathered granitoids with a soil-like behavior.

The weathering profiles observed on the gneissic cut slopes (Fig. 4) are generally complex (sensu Baynes et al., 1978) and characterized

by irregularities in the spatial distribution of weathered horizons. Fresh (class I) and slightly (class II) weathered rocks are observed along the cut slopes of the stream incisions; the medium-high portions of the slopes are mainly characterized by moderately (class III), highly (class IV) and completely (class V) weathered rocks with variable thicknesses and articulated geometric relationships (Fig. 4). The cut slopes of the highest reliefs mainly show completely weathered rocks (class V) with variable volumes of highly weathered rocks (class IV) and thin layer of residual soil (class VI). Colluvial and detrital–colluvial soils (class VI) are widespread and related to very active morphodynamic processes.

Survey of the weathering grade along the cut slopes integrated with stratigrahical analyses of the borehole logs (e.g., Borrelli et al., 2012; Calcaterra et al., 1998) allow us to evaluate the thickness and the features of the gneissic and granitoid rocks involved in the weathering processes. The borehole logs, varying from 25 to 150 m, show an irregular pattern for the weathering profiles. Based on these investigations, the weathering profiles (from classes I–II to classes V–VI) for granitoid and gneissic rocks have thickness up to 60 m (Fig. 5).

Thus, the typical weathering profiles show gradual transition from fresh/slightly weathered rock to completely weathered rock for the granitoid rocks and complex and irregular transition among the weathering classes for the gneissic rocks (Fig. 5). In particular, the upper part of the granitoid weathering profile (up to 30 m) is characterized by completely and highly weathered rocks with limited corestones of various shapes
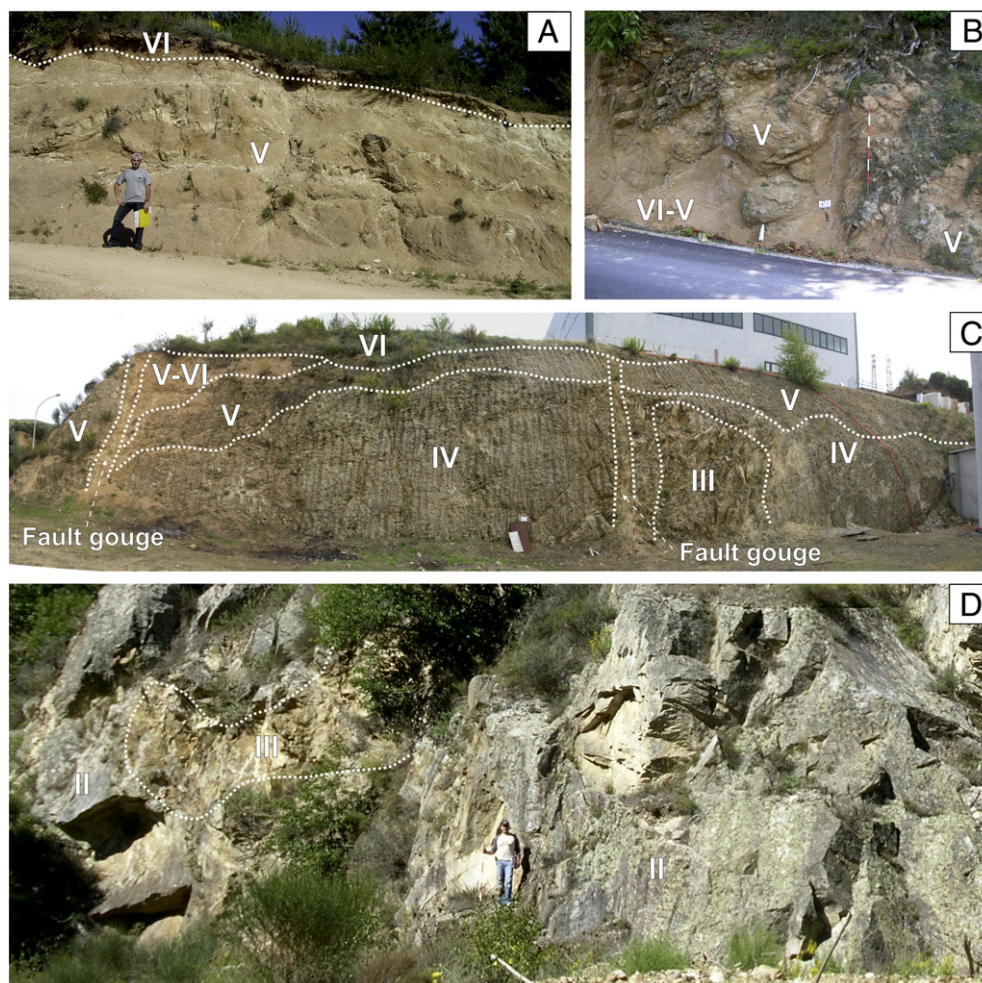
Fig. 3. Weathering profiles of representative granitoid cut slopes of the studied area: A) completely weathered rocks (class V), covered by colluvial and detritical–colluvial soils (class VI), along cut slopes of the highest reliefs; B) residual soils and completely weathered rocks (classes VI–V) with corestones (classes IV–V) along cut slopes of the highest reliefs; C) sharp contacts between different weathering classes (III, IV and V) with faults and fractured zones along the cut slopes of the medium–high portions of the slopes; D) slightly and moderately weathered rocks (classes II–III) along the cut slopes of the stream incisions.

and sizes and aplitic/pegmatitic dykes, locally covered by residual and colluvial soils (at least 5 m thick) (Fig. 5). The upper part of the gneissic weathering profile (up to 30 m) is mainly characterized by completely, highly, moderately and slightly (in minor amount) weathered rocks with various thicknesses and complex geometric relationships (Fig. 5). The medium part of the granitoid weathering profile (between 30 m and 50 m) is mainly characterized by moderately and slightly weathered rocks with aplitic/pegmatitic dykes (Fig. 5). The medium part of the gneissic weathering profile (between 30 m and 50 m) is mainly characterized by slightly, moderately and highly weathered rocks with minor amount of completely weathered rocks. The lower part of weathered profiles (down to 50 m) show similar features for both granitoid and gneissic rocks, characterized by slightly/fresh rocks (Fig. 5). The weathered profiles of gneissic rocks are generally characterized by structural complexity, such as fault gouge zones, thrust planes and joint fractures, sometimes associated to argillified levels. The weathered profiles of granitoid rocks are generally characterized by minor structural complexity (Fig. 5).

5.2. Composition of the crystalline rocks

The studied granitoid rocks are characterized by extremely different degrees and patterns of physical and/or chemical weathering. The bedrock often shows a variety of physical discontinuities, such as shear zones, fault planes, pressure release and other types of jointing, creating blocks and rounded boulders and wedges of different shapes and sizes (e.g., Borrelli et al., 2012; Scarciglia et al., 2007). These blocks are overprinted by an intense grussification, with minute rock flawing and crumbling; this forms a gritty, loose material made of small polymineral aggregates and monomineralic particles.

The granitoid rocks have a subhedral granular texture; these rocks mainly consist of strongly zoned plagioclase, anhedral quartz, biotite and chlorite. The remainder is composed of K-feldspar with accessory epidote, apatite and titanite. During the weathering a relative enrichment of quartz at the expense of feldspar has been observed (e.g., Le Pera et al., 2001a).

The gneissic rocks are mainly composed of plagioclase, quartz, biotite, iron-bearing garnet (almandine), sillimanite, muscovite and K-feldspar; minor zircon, apatite, epidote and opaques occur as accessory minerals. These rocks are medium- to coarse-grained with a grano-lepidoblastic texture. Both garnet and biotite show frequently neoformation of ferruginous weathering product as linings within and around crystals.

5.3. Petrographic analyses

Petrographic analysis based on the X_d values (Lumb, 1962) and the micropetrographic index I_p (Irfan and Dearman, 1978) have been carried out for each weathering class (Fig. 6) of the studied samples (Table 2).
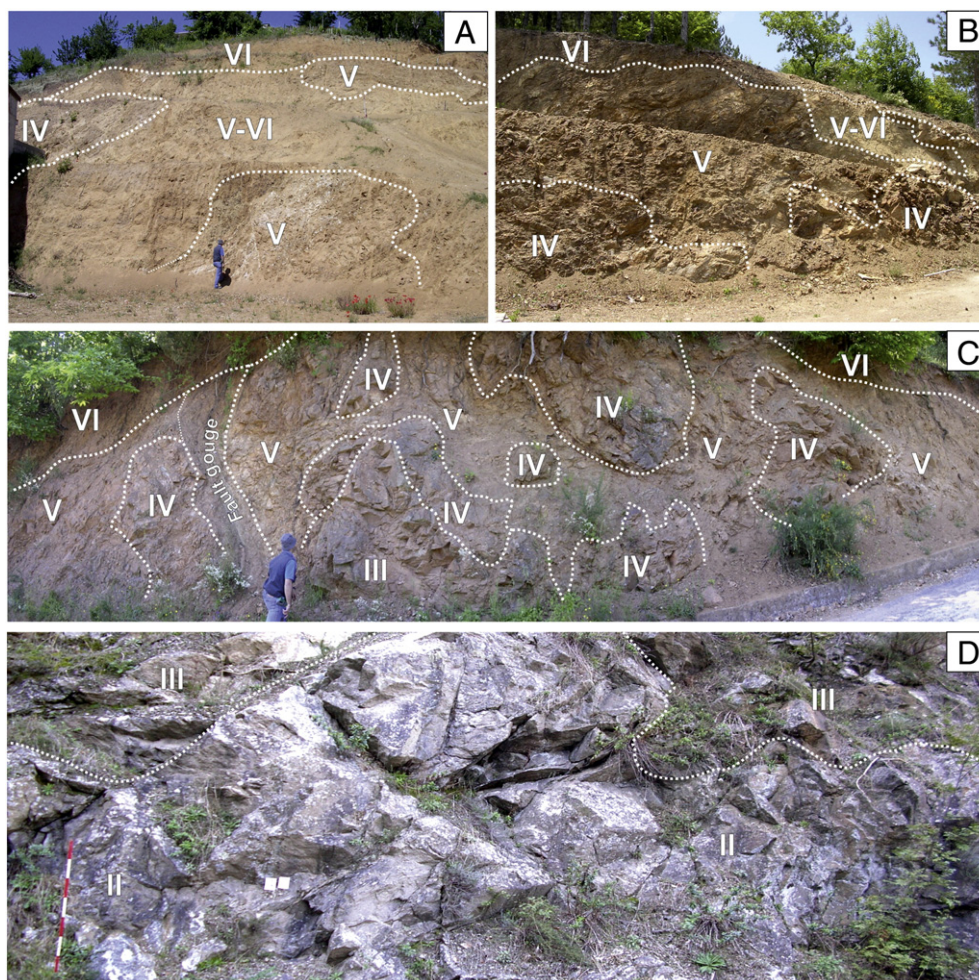
Fig. 4. Weathering profiles of representative gneissic cut slopes of the studied area: A) completely weathered rocks and residual soils (classes V–VI), with small volumes of completely weathered (class V) and highly weathered (class IV) rocks, covered by colluvial and detritical–colluvial soils (class VI), along cut slopes of the highest reliefs; B) cut slopes of the highest reliefs characterized by completely weathered rocks (class V) with variable volumes of highly weathered rocks (class IV) and thin layer of residual soil (class VI); C) cut slopes typical of the medium–high portions of the slopes characterized by moderately (class III), highly (class IV) and completely (class V) weathered rocks with variable thicknesses and articulated geometric relationships; D) slightly (class II) and moderately (class III) weathered rocks along the cut slopes of the stream incisions.

The granitoid rocks generally show low X_d values, ranging from 0.15 to 0.84 (average = 0.46), and are mainly characterized by granular-framework microfabric (Baynes and Dearman, 1978b); the granular-framework microfabric is generally clay-poor and consists of an interlocking granular aggregate enclosing decomposed minerals. Thus, referred as physical changes, the final result of weathering process is a soil-like material characterized by sand–gravel grain-size fraction for the granitoid rocks (residual soil, class VI). The granulometric analysis carried out on weathered granitoid sample (class VI), confirm that the dominant fractions are sand and gravel with minor percentage of silt–clay (Fig. 7). The micropetrographic index I_p (Irfan and Dearman, 1978) ranges from 0.27 to 14.04 related to different weathered stages (Table 1). The transition from classes I–II (Fig. 8A) to classes V–VI (Fig. 8F) consists of the sericitization of plagioclase from core to rim (for the plagioclase with an anorthitic composition), from rim to core (for the plagioclase with an albitic composition) and along preferential lines and pitting on mineral surfaces (Fig. 8B), neoformation of unidentified clay minerals within both plagioclase and K-feldspar (Fig. 8C–D), and partial clay neoformation and exfoliation of biotite along rims and lamellae (Fig. 8E–F). Transition of biotite into Fe-oxides is frequently observed (Fig. 8E–F). Generally, quartz remains unaffected by chemical alteration or shows minor modification. Starting from class III (Fig. 8C), some intragranular and intergranular small cracks, that tend to expand and propagate in the classes IV–V, can be observed (Fig. 8D–E); these weathered classes and, in

particular, the associated residual soil (classes V–VI; Fig. 8F) are characterized by open crack systems developed and filled with weathering products. Scanning electron microscope (SEM) images of completely weathered samples (class V) show evident intergranular and intra-granular cracks (Fig. 9A–B), with neoformation of clay minerals (Fig. 9C–D) and Fe-oxides (Fig. 9E) related to weathered biotite (Fig. 9F) and feldspars (Fig. 9G–H).

The gneissic rocks generally show low X_d values ranging from 0.16 to 1 (average = 0.57); the samples with highest X_d values (>0.5), show a clay-matrix microfabric (e.g., Baynes and Dearman, 1978b), typical of materials where decomposition products, mainly clayey phases, dominate and enclose the remnant original minerals. The X_d value is not detected for the fresh and the slightly weathered samples (classes I and II) (Table 2). Thus, referred as physical changes, the final result of weathering process is a soil-like material characterized by both silt–clay and sand–silt grain-size fraction for the gneissic rocks. The granulometric analysis, carried out on weathered gneissic sample (class VI), confirms that the dominant fractions are sand and silt–clay with minor percentage of gravel (Fig. 7). The micropetrographic index I_p (Irfan and Dearman, 1978) ranges from 0.25 to 14.17 related to different weathered stages (Table 2). The transition from class I (Fig. 10A) to class VI (Fig. 10F) is mainly related to pervasive sericitization of plagioclase and pitting on mineral surfaces (Fig. 10C–D), incipient weathering of plagioclase rims and clay coating of altered grains (Fig. 10D), and
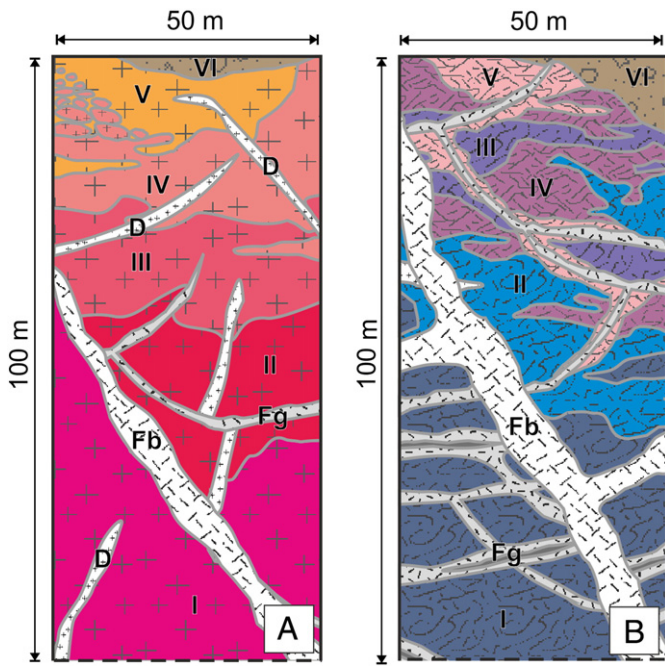
Fig. 5. Typical weathering profiles of (A) granitoid and (B) gneissic rocks for the study area. VI, residual and colluvial soil; V, completely weathered rock; IV, highly weathered rock; III, moderately weathered rock; II, slightly weathered rock; I, fresh rock; D, aplitic–pegmatitic dike; Fg, fault gouge; Fb, fault breccia.

neoformation of clay filling the microcracks (Fig. 10E). Completely weathered feldspar and biotite grains are replaced by clay minerals and Fe-oxides, and embedded in an oxidized argillaceous matrix (Fig. 10E–F). Scanning electron microscope (SEM) images of completely weathered samples (class V) show intergranular and intragranular cracks (Fig. 11A), formation of clay coating on weathered grains (Fig. 11B–C), altered and exfoliated biotite replaced by Fe-oxide (Fig. 11D–E) and neoformed clay minerals (e.g., halloysite, kaolinite, illite and mixed-layer clay minerals) (Fig. 11F–H). In detail, SEM-EDS observations show thin 2–6 μm minerals

(Fig. 11F–H); these phases are probably halloysite crystals growing with their long axes perpendicular to the plagioclase grains (Fig. 11G) and rare pseudohexagonal lamellae of kaolinite (Fig. 11F) and mica mixed-layers (Fig. 11H), as indicated by EDS analyses (data not shown).

5.4. Mineralogical analyses

The X-ray diffraction pattern of the completely weathered samples (of both granitoid and gneissic rocks) shows the occurrence of neoformed clay minerals, typically large amounts of interstratified clay minerals (both 2:1 and 2:1:1 clay minerals), chlorite, micas and 1:1 clay minerals (Fig. 12). The difference between granitoid and gneissic rocks is mainly related to a higher content of quartz and feldspars for the first rock type (Fig. 12A) whereas the second rock type shows higher content of neoformed clay minerals (Fig. 12B). The XRD pattern of the granitoid rock clay fraction shows quartz and feldspars peaks more intense than the same peaks of the gneissic rock, characterized by higher content of neoformed clay minerals (Fig. 12). These mineralogical differences between the completely weathered studied rocks have a correspondence also in the mineralogical investigation of the <2 μm fraction. The XRD patterns of the <2 μm fraction, show high content of clay minerals mainly constituted by expandable phases (mixed-layer minerals) (Fig. 13); in particular, the gneissic sample (Fig. 13B) shows higher variations among the treated specimens (air dried, glycolated and heated) at low-angle related to the abundance of expandable phases, rather than the granitoid sample (Fig. 13A). These observations confirm the minero-petrographic and granulometric analyses.

6. The effect of weathering processes

Based on guidelines given in earlier studies, we assessed physical, chemical and minero-petrographical features of the weathering process (e.g., Baynes and Dearman, 1978a, b; Borrelli et al., 2007, 2012; Caracciolo et al., 2011; Critelli et al., 2008; Gullà and Matano, 1997; Irfan and Dearman, 1978; Le Pera and Sorriso-Valvo, 2000a,b; Le Pera et al., 2001b; Lee and De Freitas, 1989; Lumb, 1962; Mongelli et al., 2006; Perri, 2011; Perri et al., 2008, 2011a,b, 2012, 2013; Scarciglia et al., 2005, 2007; Zaghloul et al., 2010).
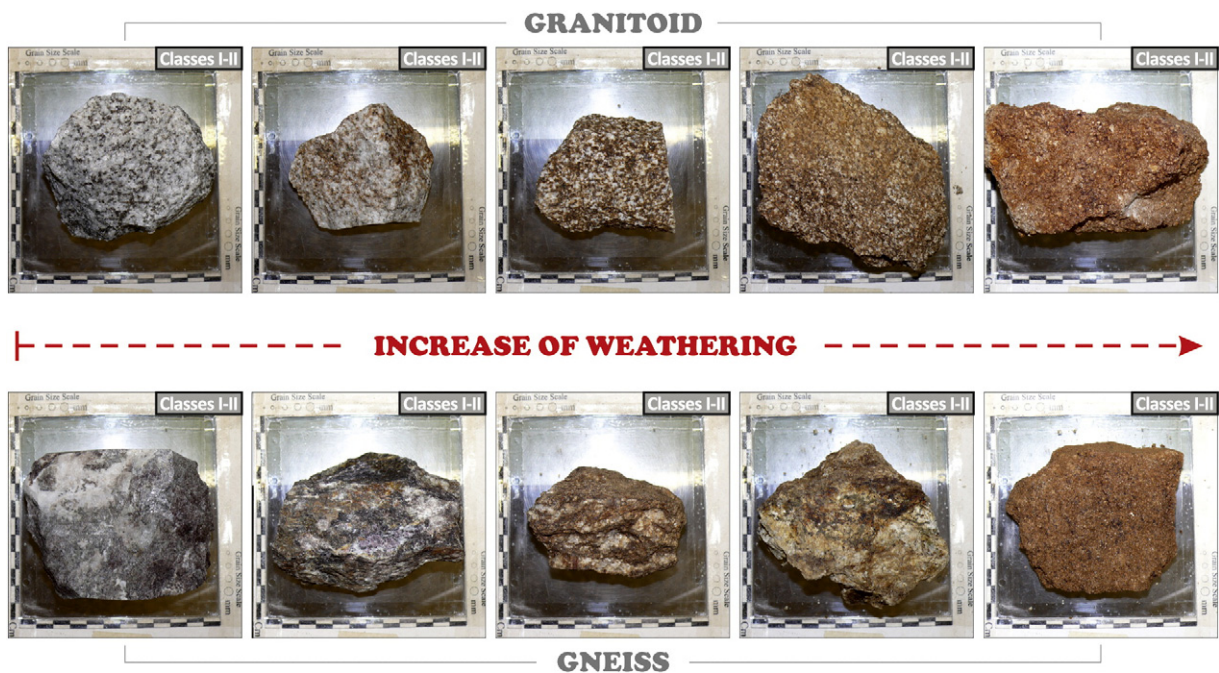
Fig. 6. Granitoid and gneissic rock samples representative of each stage of weathering.

Table 2
Characterization of studied granitoid and gneiss in terms of decomposition index (X_d; Lumb, 1962), microfabric (Baynes and Dearman, 1978b), micropetrographic index (I_p; Irfan and Dearman, 1978) and weathering stage. C, samples from cut slopes; S1A, samples from borehole.

Sample	Type of rock	Decomposition index (X_d)	Microfabric	Unaltered minerals (%)	Altered minerals (%)	Microfracture and void (%)	Micropetrographic index (I_p)	Weathering stage
C1	Gneiss	–	Granular-framework	82.97	16.76	0.27	4.87	III
C2	Gneiss	0.38	Granular-framework	74.91	22.81	2.28	2.99	IV
C6	Gneiss	–	Granular-framework	93.89	7.11	0	13.06	I
C14	Gneiss	–	Granular-framework	88.47	10.87	0.66	7.67	II
C24	Gneiss	–	Granular-framework	82.92	16.18	0.9	4.85	III
C43	Gneiss	0.51	Clay-matrix	66.15	20.47	14.33	1.9	IV–V
C44	Gneiss	0.56	Clay-matrix	46.77	44.62	8.61	0.88	V
C84	Gneiss	0.26	Granular-framework	73.71	18.69	7.6	2.8	IV
SIA-1	Gneiss	0.16	Granular-framework	80.8	18.28	0.92	4.21	III
SIA-2	Gneiss	0.39	Granular-framework	76.84	17.49	5.67	3.32	IV
SIA-3	Gneiss	0.18	Granular-framework	74.45	24.19	1.36	2.91	IV
SIA-4	Gneiss	–	Granular-framework	93.35	6.07	0.58	14.04	I
C18	Gneiss	0.92	Clay-matrix	19.85	70.35	9.8	0.25	V
C28	Gneiss	0.55	Clay-matrix	29.92	44.27	25.81	0.43	V
C31	Gneiss	1	Clay-matrix	39.41	57.29	3.3	0.65	V
C32	Gneiss	0.93	Clay-matrix	42.3	45.68	12.02	0.73	V
C39	Gneiss	0.79	Clay-matrix	23.95	56.96	19.09	0.31	V
C62	Gneiss	0.21	Granular-framework	67.99	25.27	6.74	2.12	IV
C78	Gneiss	–	Granular-framework	93.41	6.1	0.49	14.17	I
C81	Gneiss	–	Granular-framework	86.35	12.47	1.18	6.33	II
C94	Gneiss	–	Granular-framework	92.46	7.29	0.25	12.26	I
C95	Gneiss	0.97	Clay-matrix	27.94	62.09	9.97	0.39	V–VI
C98	Gneiss	0.48	Clay-matrix	40.52	40.33	10.15	0.68	V–VI
C107	Gneiss	0.85	Clay-matrix	58.42	31.01	1.45	1.8	IV–V
C57	Granitoid	–	Granular-framework	89.2	9.56	0.52	8.26	II
C60	Granitoid	0.4	Granular-framework	64.13	19.14	16.73	1.79	V
C64	Granitoid	–	Granular-framework	80.96	16.29	2.75	4.25	III
C72	Granitoid	0.84	Clay-matrix	61.2	32.68	6.12	1.57	V
C74	Granitoid	0.8	Clay-matrix	21.29	64.84	13.87	0.27	V–VI
C77	Granitoid	0.33	Granular-framework	42.17	43.77	14.06	0.73	V–VI
C89	Granitoid	0.42	Granular-framework	59.05	29.14	11.81	1.44	V
C102	Granitoid	–	Granular-framework	91.83	7.92	0.25	11.24	II–I
C103	Granitoid	–	Granular-framework	82.35	14.58	3.07	4.67	III
C104	Granitoid	0.15	Granular-framework	42.83	36.2	20.97	0.75	V
C105	Granitoid	0.28	Granular-framework	69.2	23.15	7.65	2.24	V–IV

The main features of the weathered granitoid and gneissic rocks are shown in Table 1, based on macroscale observations. Generally, fresh rock (class I) is unchanged from original state; slightly weathered rock (class II) shows same color of the fresh rock (class I) with discoloration only close to the discontinuities; original texture and microstructure of the fresh rock are preserved. Moderately weathered rock (class III) is pervasively discolored, but the color of the fresh rock is locally observed. The original texture and microstructure of the fresh rock are well preserved. Highly weathered rock (class IV) is completely discolored; original texture and microstructure of the fresh rock are still preserved. Completely weathered rock (class V) is also completely discolored; original texture and microstructure of the fresh rock are present in relict form. Residual and colluvial soils (class VI) are respectively constituted from soil related to in situ weathering and soil reworked and transported by colluvial–detrital processes; original texture and microstructure of the fresh rock are completely destroyed.

The main weathered minerals observed in the studied samples from granitoid and gneissic weathering profiles are plagioclase, biotite and potassium feldspar (Fig. 14), as shown by thin section, SEM and XRD analyses. Fine-grained sericite often occurs within plagioclase during the incipient weathering stages (classes II–III), preferentially along twin planes, or more pervasively. A pre-weathering origin for sericite has been considered (Dixon and Young, 1981; James et al., 1981; Velbel, 1983), even if a formation during deep weathering conditions cannot be ruled out (Irfan and Dearman, 1978; Ollier, 1983, 1984, 1988). As weathering advances (starting from class IV) clay minerals replace fine-grained sericite, preferentially along mineral rims and intragranular microfractures (Fig. 14A). Neoformed mixed-layer clay minerals are major constituents of altered biotite grains from each horizon of the profiles; illite, illite–smectite mixed layers, kaolinite and halloysite are also present in various amounts as shown by XRD analyses. Unaltered biotite is present in some specimens in association with mixed-layer clay minerals and probably represents both unaltered biotite grains and biotite cores of weathered grains. Under natural weathering conditions, changes in the nature of octahedral cations in biotite are usually associated with replacement of K^+ by hydrated cations. Biotite crystals are exfoliated, and show frequently etched, outer boundaries (sometimes with clay neoformation and Fe-oxide staining) and may separate along cleavage lines (Fig. 14B–D). Oxidation probably preceded or accompanied K-exchange from biotite in these profiles (e.g., Gilkes and Suddhiprakarn, 1979). The advanced stage of weathering (classes V–VI) is marked by chemical breakdown and weathering of potassium feldspar (Fig. 14E). These samples (classes V–VI) are characterized by fractured quartz grains (Fig. 14F) that usually form the skeleton of saprolite in an argillaceous matrix, with the detrital feldspars and micas.

Halloysite and kaolinite may often coexist in the upper parts of the gneissic and granitoid weathering profiles (classes V–VI) developed under a temperate climate (e.g., Papoulis et al., 2004), as the Mediterranean environment. Chlorite forms under a variety of physical and chemical weathering conditions (e.g., Weaver, 1989). Illite mainly exists in areas of very low rates of chemical weathering with cooler climate, and areas of steep relief where mechanical erosion interferes with soil formation (e.g., Weaver, 1989).

Thus, the granitoid and gneissic rocks show similar features for the fresh, slightly and moderately weathered rocks (classes I–III) at macro- and microscale, whereas they are characterized by a different response to the weathering processes starting from highly weathered rocks (class IV). In particular, many gneissic samples (classes V–VI) are characterized by higher percentage of altered minerals rather than few granitoid (classes V–VI) samples (Table 2), as well as the microfracture and
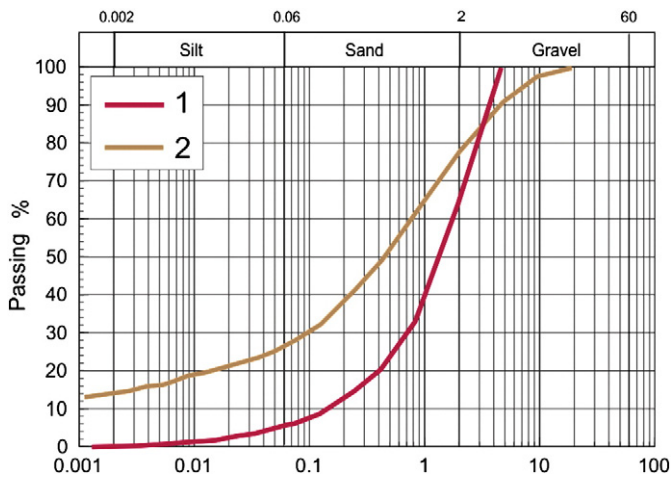
Fig. 7. Grain size distribution curves of the residual soils (class VI): (1) granitoid sample (C74; Table 2); (2) gneissic sample (C95; Table 2).

void percentage is higher in many gneissic samples (classes V–VI) rather than in few granitoids (classes V–VI). Furthermore, the percentage of the gneissic samples (classes V–VI) characterized by clay-matrix microfabric is higher than those of the granitoid samples (classes V–VI), mainly characterized by granular-framework microfabric. This generally produces a greater value of the Sand Generation Index (SGI; Palomares and Arribas, 1993) for granitoids and explains the great productivity in sandy deposits of this lithology.

7. Concluding remarks

This work concerns the importance and the great potential of combining complementary scientific disciplines to the study of weathering profiles and the derivative products. Both physical and chemical weathering affect granitoid and gneissic rocks of the Sila Massif (Calabria, southern Italy), where the combination of tectonic and climate variation plays an important key role.

Although chemical weathering seems to be the dominant process, fracturing and faulting are also crucial factors in the development of
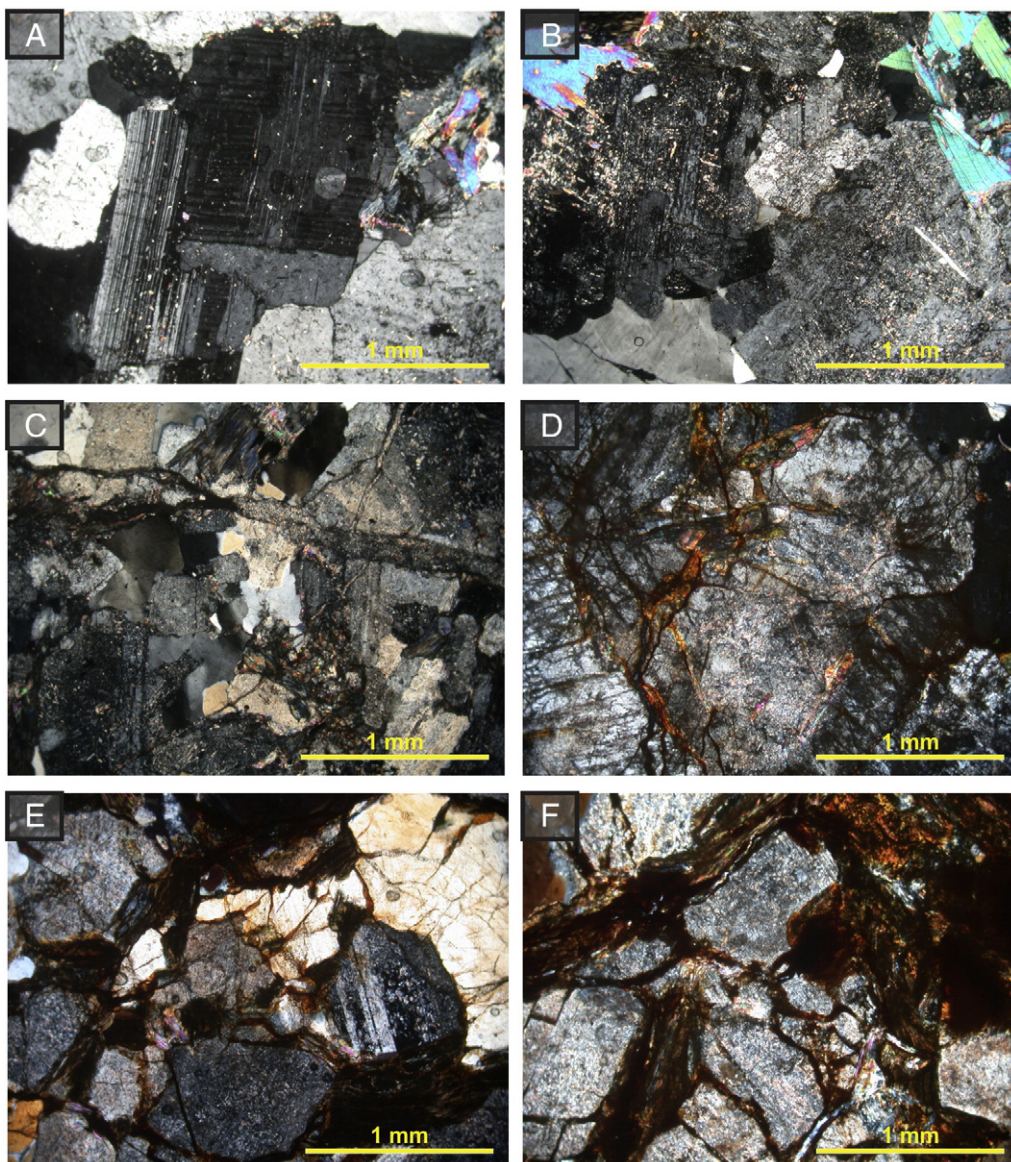

Fig. 8. Photomicrographs of weathering stages for the studied granitoid (crossed polarized light; 10×). A) Fresh rock (class I); B) slightly weathered sample (class II); C) moderately weathered sample (class III); D) highly weathered sample (class IV); E) completely weathered sample (class V); F) completely weathered sample characterized by clasts in an oxidized argillaceous matrix (classes V–VI).
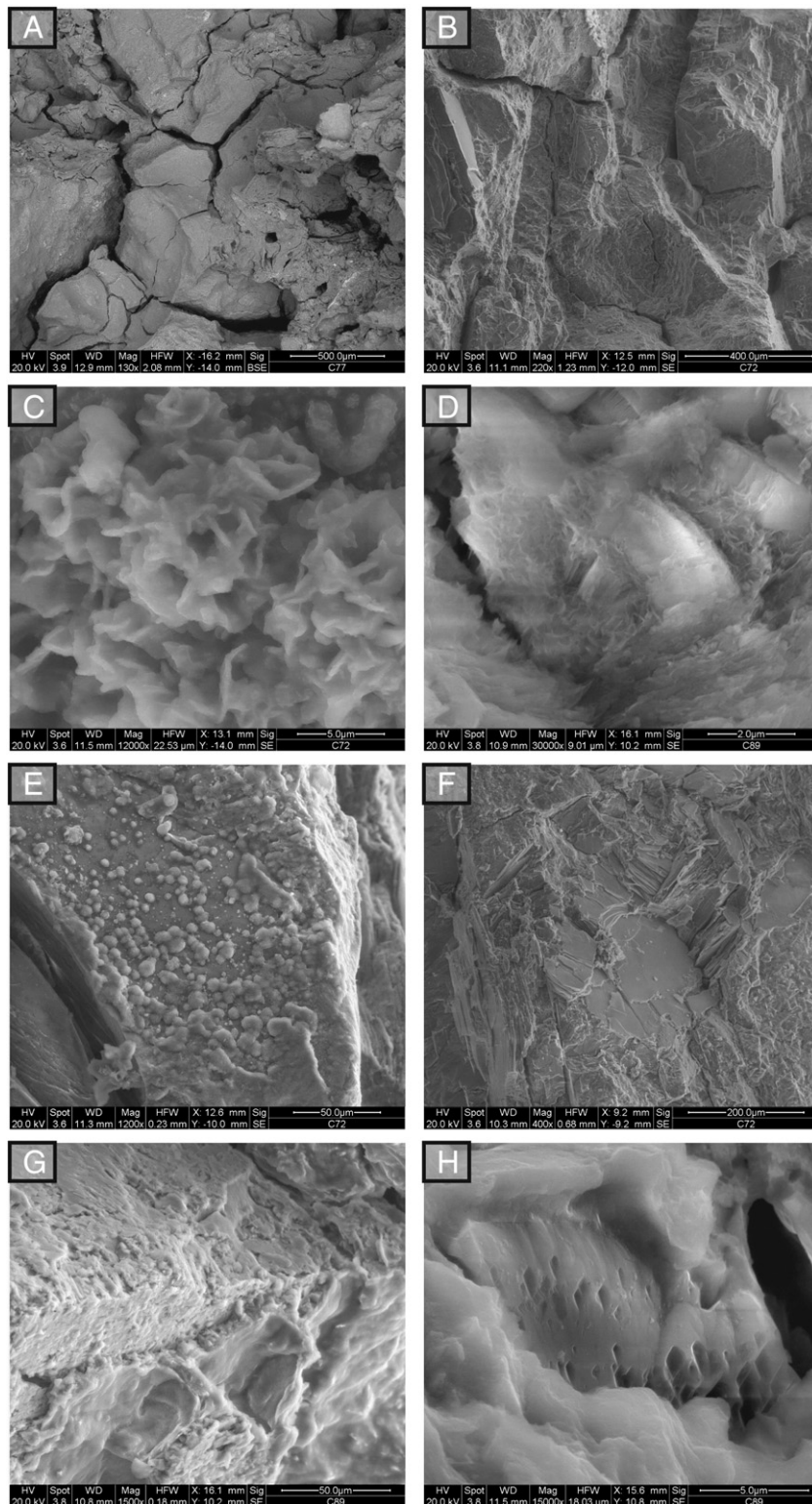
Fig. 9. Scanning electron microscope photographs of granitoid rocks. A) Structure; B) incipient disintegration testified by transgranular and intragranular microcracks; C) argillification (neoformed clay minerals) of plagioclase; D) booklets of kaolinite; E) quartz covered by Fe-oxides; F) exfoliated biotite, partially replaced by Fe-oxides; G) neoformed clay mineral coating plagioclase crystal; H) chemical alteration of feldspar grain characterized by pitting phenomena.

granitoid and gneissic weathering profiles. Weathered rock masses have been estimated to be at least 60 m in thicknesses. The development of these weathering profiles is thought to have occurred between the Late Miocene and Pleistocene. Under the current temperate and Pleistocene glacial climatic conditions, the erosional processes, as activated by tectonic uplifting of the north-western slopes of the Sila Massif,

have partially removed the exposed deeply weathered mantle; the last is mainly confirmed by field observation and evaluation of the cut slope weathering profiles.

Petrographic and mineralogical analyses show characteristic changes as weathering progresses. The weathering stage transitions are well documented by X_d values and the micropetrographic index I_p
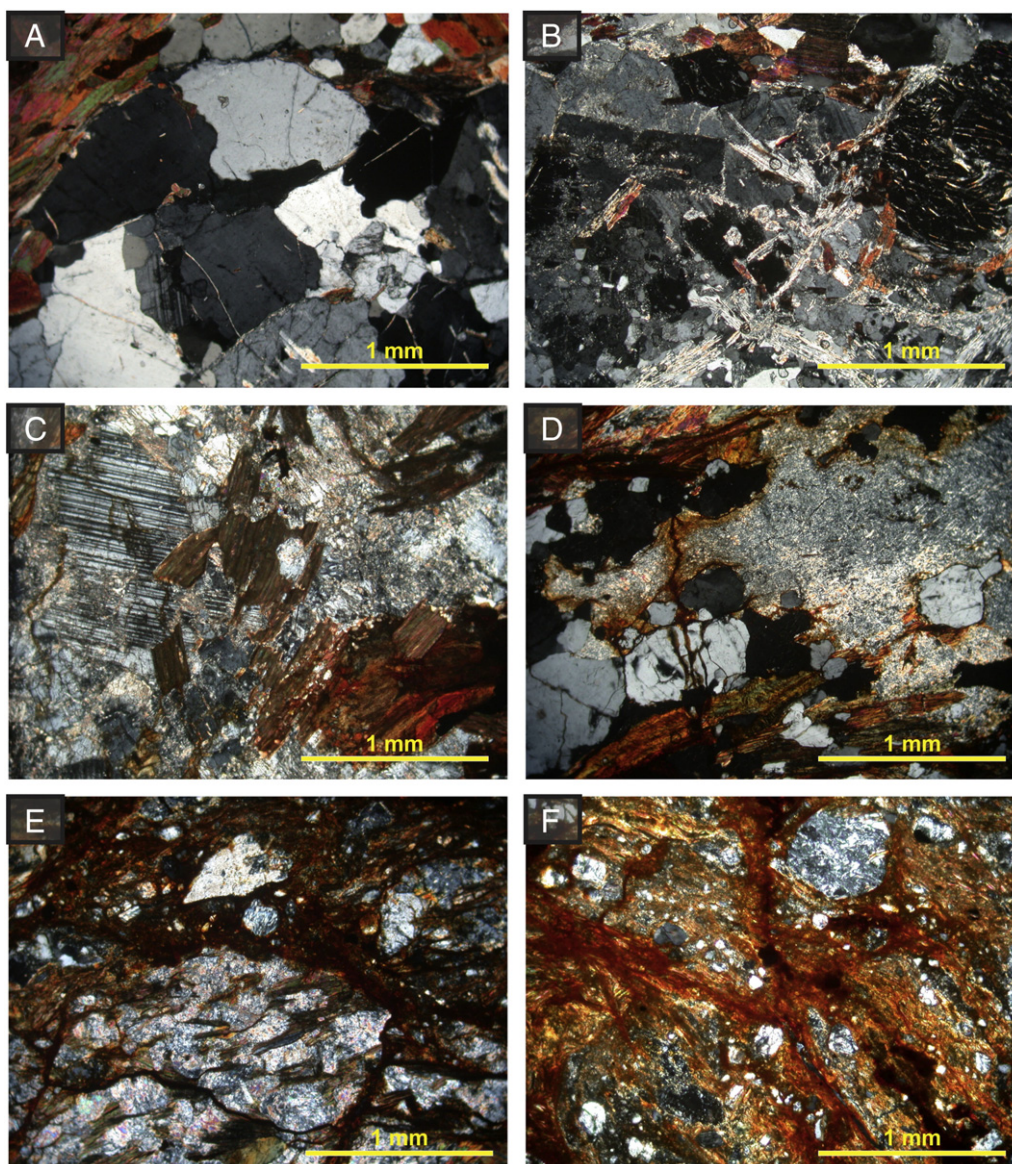
Fig. 10. Photomicrographs of weathering stages for the studied gneiss (crossed polarized light; 10×). A) Fresh rock (class I); B) slightly weathered sample (class II); C) moderately weathered sample (class III); D) highly weathered sample (class IV); E) completely weathered sample (class V); F) residual soil sample characterized by abundant and rounded clasts in an oxidized and argillaceous (clay) matrix (class VI).

and by SEM and thin-section images and XRD patterns. The formation of microcracks and the mineralogical transformations (e.g., neoformed clay minerals) can lead to a significant reduction in the effective shear strength and stiffness of the granitoid and gneissic masses and play an important role in the development of different types of widespread slope instability in the studied area. Generally, shallow landslide (e.g. slide and flow slide, up to 3 m deep) involve soil-like materials in the granitoid and gneissic weathering profiles (class VI and class V); medium-deep landslide (e.g. slide, up to 30 m deep) involve soil-like rocks and weak rocks in the granitoid and gneissic weathering profiles (class VI, class V, and class IV); deep landslide (e.g. rock slide, greater than 30 m deep) and DSGSD (Deep Seated Gravitational Slope Deformation) involve the fresher rocks (class III, class II and class I) in the gneissic weathering profiles, where fault rocks (fault breccia and fault gouge zone) are present (e.g., Borrelli et al., 2007, 2012; Calcaterra and Parise, 2010; Cascini et al., 1992 and references therein).

The approach used and the results proposed in this paper may provide a valuable support for the study of typical mass movement phenomena related to different geological contexts mainly characterized by weathered crystalline rocks, and for the mechanical characterization of weathering profiles for engineering geological investigations. In addition, this study generates crucial information concerning the first step in sediment generation, as the control of lithology at the sources and their behavior in sediment production as an original product from weathering profiles.
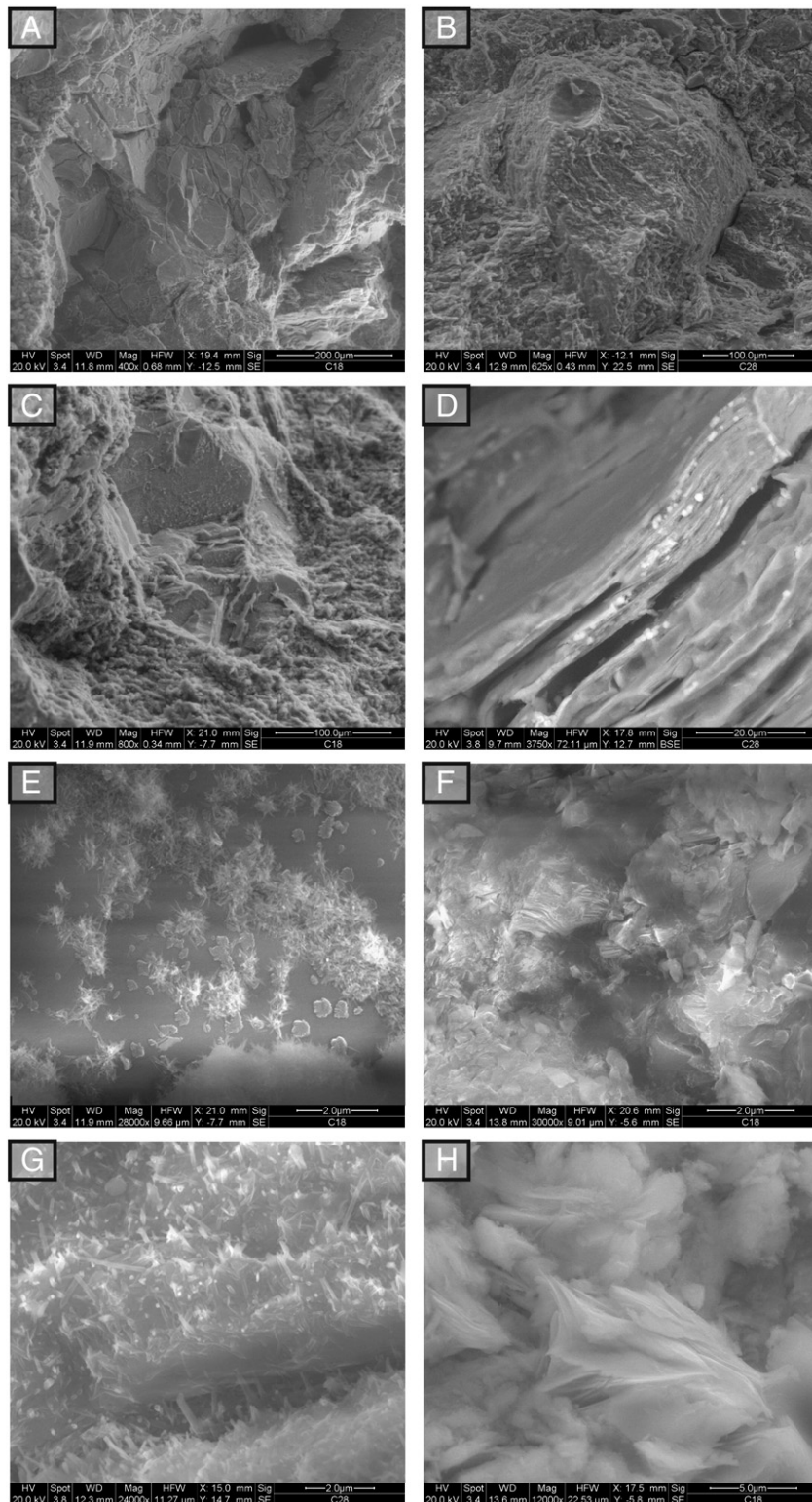
**Fig. 11.** Scanning electron microscope photographs of gneissic rocks. A) Incipient disintegration testified by transgranular and intragranular microcracks; B) plagioclase grain in an argillaceous matrix; C) biotite replaced by Fe-oxides; D) weathered biotite crystal with exfoliation occurring along cleavage lines; E) quartz covered by Fe-oxides; F) booklets of kaolinite; G) thin minerals constituted by halloysite crystals; H) neoformed clay minerals (platy illite).

References

Baynes, F.J., Dearman, W.R., 1978a. The microfabric of a chemically weathered granite. Bull. Int. Assoc. Eng. Geol. 18, 91–100.

Baynes, F.J., Dearman, W.R., 1978b. The relationship between the microfabric and the engineering properties of weathered granite. Bull. Int. Assoc. Eng. Geol. 18, 191–197.

Baynes, F.J., Dearman, W.R., Irfan, T.Y., 1978. Practical assessment of grade in a weathered granite. Bull. Int. Assoc. Eng. Geol. 18, 101–109.

Bonardi, G., Cavazza, W., Perrone, V., Rossi, S., 2001. Calabria–Peloritani Terrane and Northern Ionian Sea. In: Vai, G.B., Martini, I.P. (Eds.), Anatomy of an Orogen: The Apennines and Adjacent Mediterranean Basins. Kluwer Academic Publishers, Dordrecht/Boston/London, pp. 287–306.
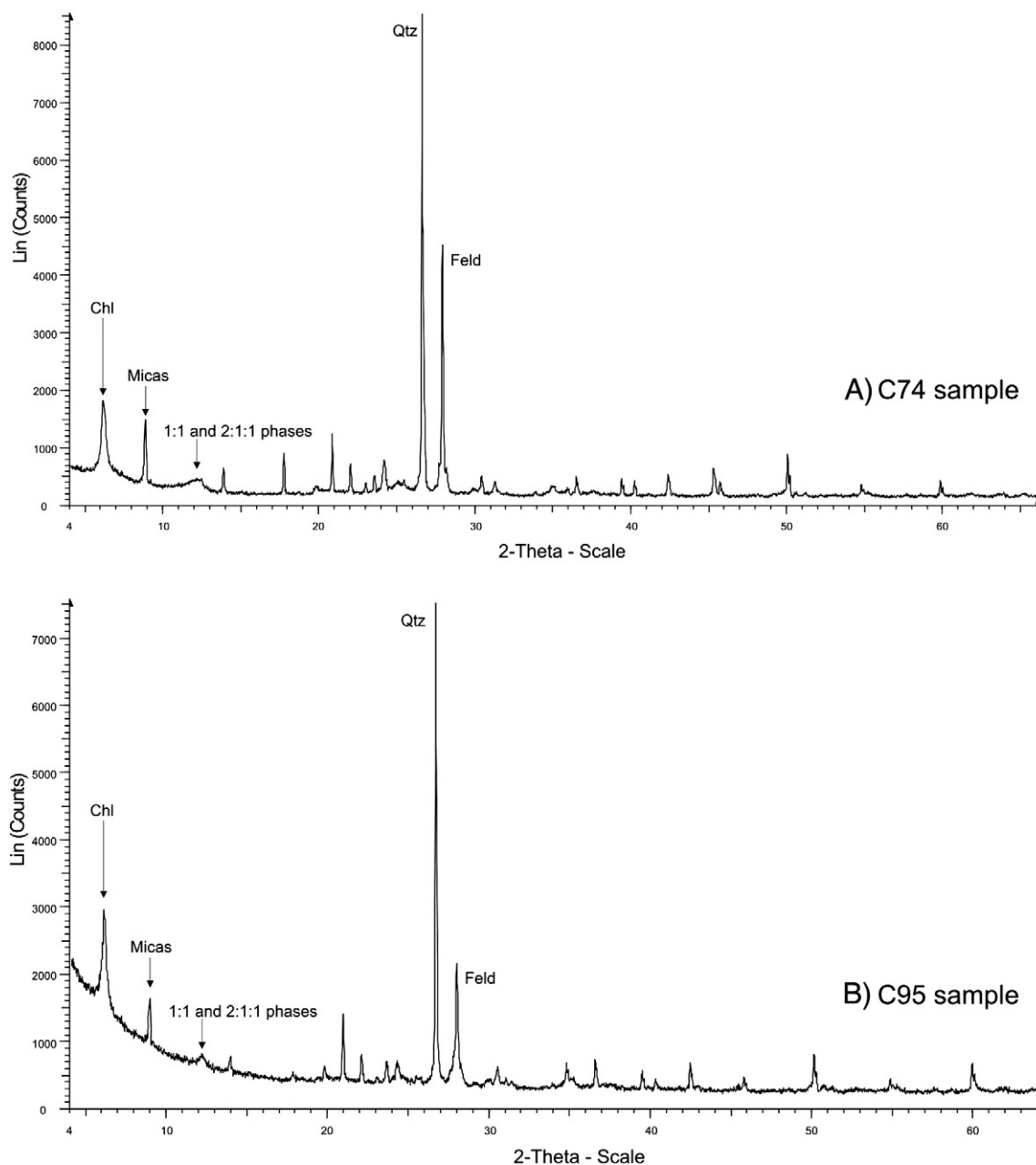
Fig. 12. X-ray diffraction patterns for (A) completely weathered granitoid (C74; Table 2) and (B) completely weathered gneissic (C95; Table 2) bulk samples. Qtz, quartz; Feld, feldspars; Chl, chlorite.

Borrelli, L, 2008. Categorie di frane ed elementi caratteristici nei profili di alterazione. Ph.D. Thesis University of Calabria, Italy.

Borrelli, L., Greco, R., Gullà, G., 2007. Weathering grade of rock masses as a predisposing factor to slope instabilities: reconnaissance and control procedure. Geomorphology 87, 158–175.

Borrelli, L, Critelli, S., Gullà, G., Muto, F., 2011a. Weathering grade and mass movements map of the Mucone river basin west-central side (Calabria, Italia). Litografia Artistica Cartografica.Firenze, Italy.

Borrelli, L., Critelli, S., Gullà, G., Muto, F., 2011b. Rilievo del grado di alterazione di rocce cristalline. Presentazione della "Carta del grado di alterazione e dei movimenti in massa della porzione centro-occidentale del bacino del F. Mucone (Calabria, Italia)". Anno 11, Numero SpecialeGeologi Calabria 3–46.

Borrelli, L., Perri, F., Critelli, S., Gullà, G., 2012. Minero-petrographical features of weathering profiles in Calabria, southern Italy. Catena 92, 196–207.

Brand, E.W., Phillipson, H.B., 1985. Sampling and testing of residual soils: a review of international practice. Technical Committee on Sampling and Testing of Residual Soils. International Society for Soil Mechanics and Foundation EngineeringScorpion Press 1–194.

Calcaterra, D., Parise, M., 2010. Weathering in the crystalline rocks of Calabria, Italy, and relationships to landslides. In: Calcaterra, D., Parise, M. (Eds.), Weathering as a Predisposing Factor to Slope Movements. Geological Society of London, 23. Engineering Geology Special Publication, pp. 105–130.

Calcaterra, D., Parise, M., Dattola, L., 1998. Weathering processes in crystalline rocks of the Sila Massif, Calabria, southern Italy, as predisposing factor for the development of debris flows. In: Evangelista, A., Picarelli, L. (Eds.), The Geotechnics of Hard Soils. Balkema, Rotterdam, pp. 73–84.

Caracciolo, L., Le Pera, E., Muto, F., Perri, F., 2011. Sandstone petrology and mudstone geochemistry of the Peruc–Korycany Formation (Bohemien Cretaceous Basin, Czech Republic). Int. Geol. Rev. 53, 1003–1031.

Cascini, L., Gullà, G., 1993. Caratterizzazione fisico-meccanica dei terreni prodotti dall'alterazione di rocce gneissiche. Riv. Ital. Geotec. 2, 125–147.

Cascini, L., Critelli, S., Di Nocera, S., Gulla, G., Matano, F., 1992. Grado di alterazione e franosità negli gneiss del massiccio silano: l'area di San Pietro in Guarano (CS). Geol. Appl. Idrogeol. 27, 49–76.

Cascini, L., Critelli, S., Di Nocera, S., Gullà, G., Matano, F., 1994. Weathering and landsliding in Sila Massif gneiss (Northern Calabria, Italy). Proceedings of the 7th International IAEG Congress. Lisboa, Portugal, pp. 1613–1622.

Corbi, F., Fubelli, G., Lucà, F., Muto, F., Pelle, T., Robustelli, G., Scarciglia, F., Dramis, F., 2009. Vertical movements in the Ionian margin of the Sila Massif (Calabria, Italy). Boll. Soc. Geol. 128, 731–738.
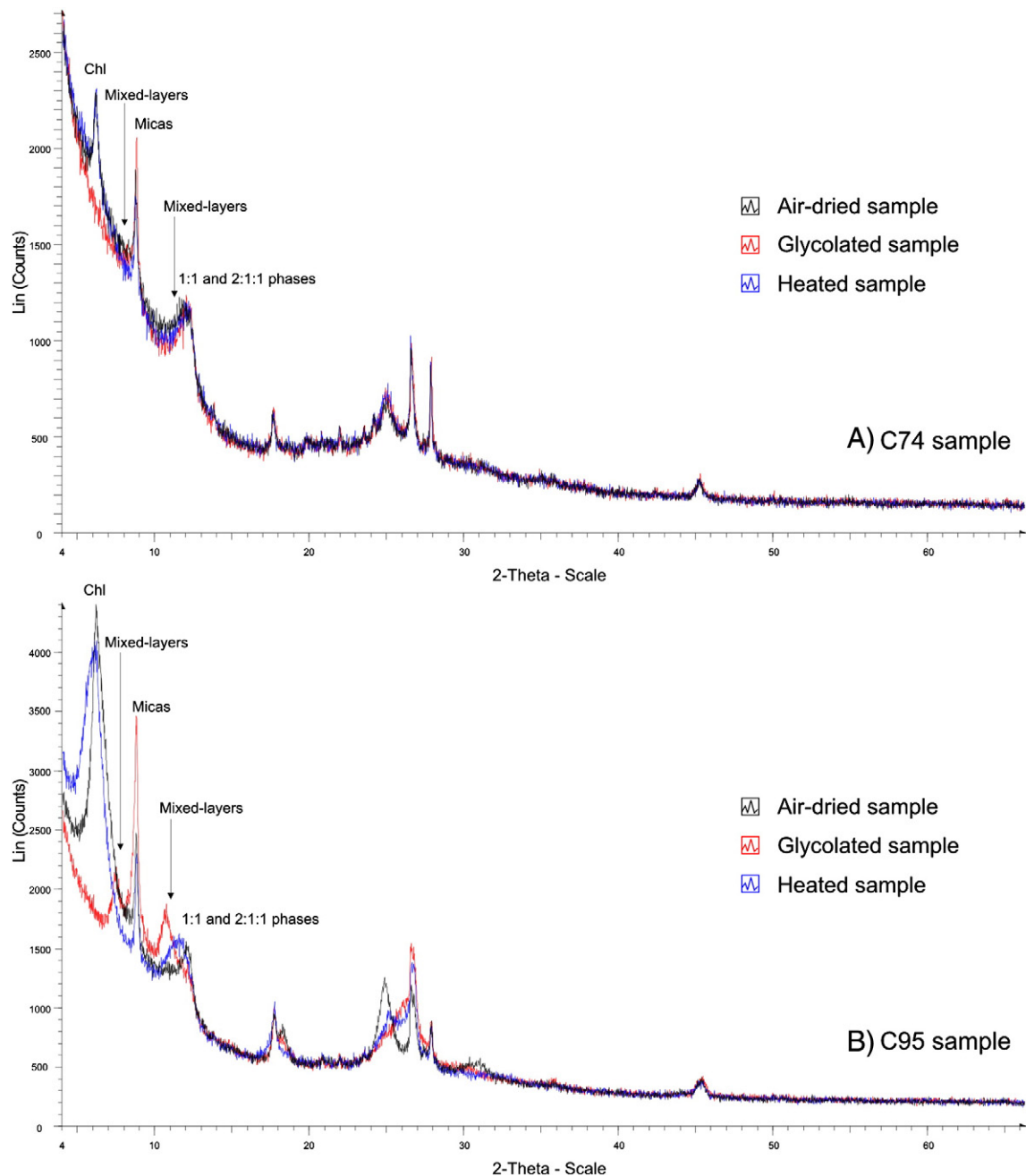
Fig. 13. X-ray diffraction patterns of <2 μm treated specimens (air dried, glycolated and heated). (A) Completely weathered granotoid (C74; Table 2) and (B) completely weathered gneiss (C95; Table 2).

Critelli, S., Di Nocera, S., Le Pera, E., 1991. Approccio metodologico per la valutazione petrografica del grado di alterazione degli gneiss del Massiccio Silano (Calabria settentrionale). Geol. Appl. Idrogeol. 26, 41–70.

Critelli, S., Mongelli, G., Perri, F., Martìn-Algarra, A., Martìn-Martìn, M., Perrone, V., Dominici, R., Sonnino, M., Zaghloul, M.N., 2008. Compositional and geochemical signatures for the sedimentary evolution of the Middle Triassic–Lower Jurassic continental redbeds from Western-Central Mediterranean Alpine Chains. J. Geol. 116, 375–386.

Deere, D.U., Patton, F.D., 1971. Slope stability in residual soils. Proceedings of the 4th Pan American Conference on Soil Mechanics and Foundation Engineering. San Juan, Puerto Rico, pp. 87–170.

Dixon, J.C., Young, R.W., 1981. Character and origin of deep arenaceous weathering mantles on the Bega Batholith, southeastern Australia. Catena 8, 97–109.

Garfì, G., Bruno, D.E., Calcaterra, D., Parise, M., 2007. Fan morphodynamics and slope instability in the Mucone River basin (Sila Massif, southern Italy): significance of weathering and role of land use changes. Catena 69, 181–196.

Geological Society Engineering Group Working Party (G.S.E.G.W.P.), 1995. The description and classification of weathered rocks for engineering purposes. Q. J. Eng. Geol. 28, 207–242.

Gilkes, R.J., Suddhiprakarn, A., 1979. Biotite alteration in deeply weathered granite. I. Morphological, mineralogical, and chemical properties. Clays Clay Miner. 27, 349–360.

Gullà, G., Matano, F., 1997. Surveys of weathering profile on gneiss cutslopes in Northern Calabria, Italy. Proceedings of the International Symposium on Engineering Geology and the Environment, IAEG. Athens, Greek, pp. 133–138.

Gullà, G., Borrelli, L, Greco, R., 2004. Weathering of rock-mass as possible characterizing factor of predisposition to slope instabilities. Proceedings of the IX International Symposium on Landslides. Rio de Janeiro, Brazil, pp. 103–108.

Guzzetta, G., 1974. Ancient tropical weathering in Calabria. Nature 251, 302–303.

Ietto, A., Ietto, F., 2004. Age and history of the weathering of granitoids in southern Calabria. Geogr. Fis. Din. Quat. 27, 37–45.

Irfan, T.Y., Dearman, W.R., 1978. The engineering petrography of a weathered granite in Cornwall. Engl. Q. J. Eng. Geol. 11, 223–244.

James, W.C., Mack, G.H., Suttner, L.J., 1981. Relative alteration of microcline and sodic plagioclase in semi-arid and humid climates. J. Sediment. Petrol. 51, 151–164.

Köppen, W., 1936. Das geographische System der Klimate. In: Köppen, W., Geiger, R. (Eds.), Handbuch der Klimatologie. Band 5. Gebrüder Bornträger, Berlin, pp. 1–46 (Teil C).
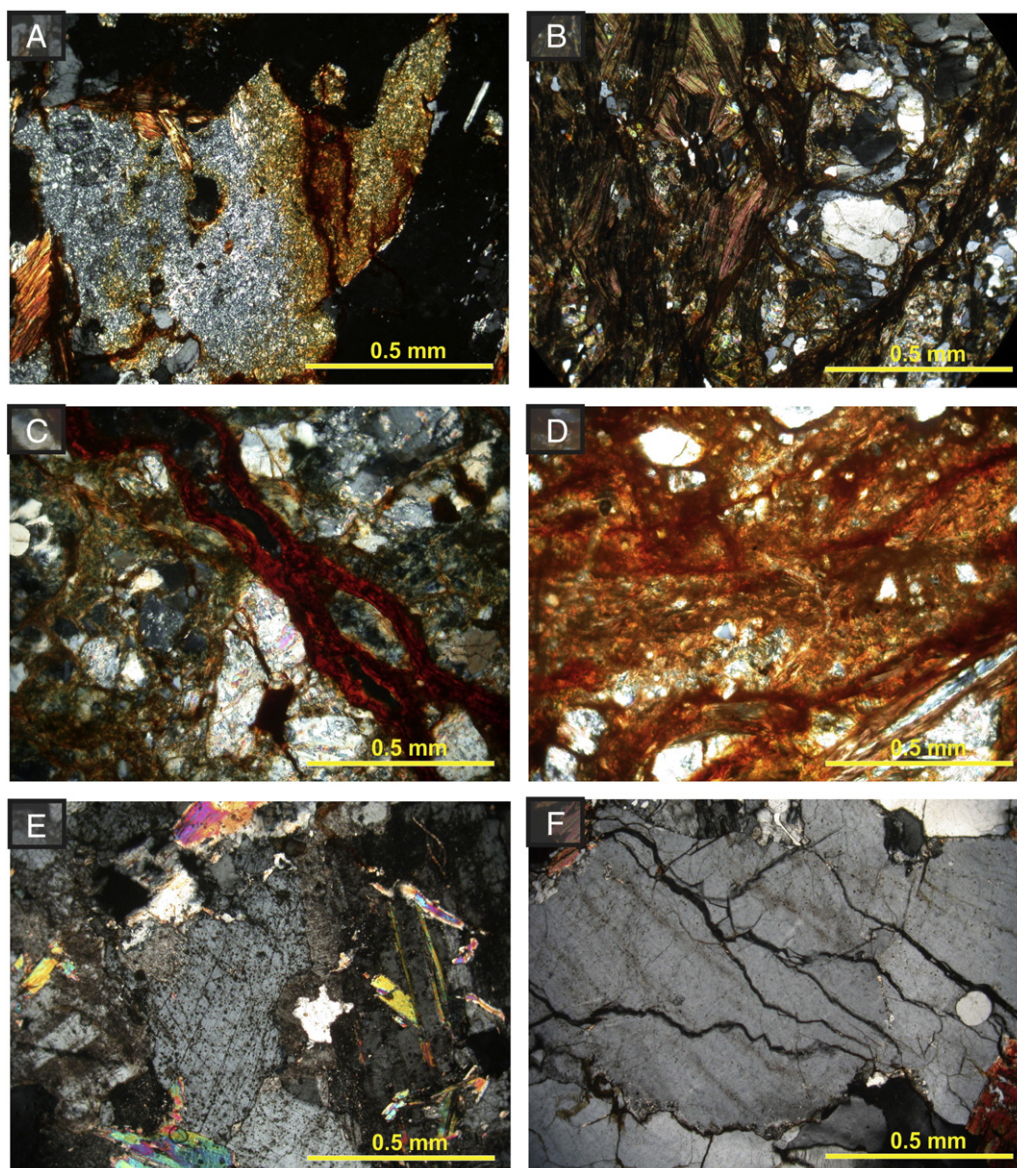
Fig. 14. Stages of main mineral alteration (crossed polarized light; 20×). A) Advanced stage of plagioclase alteration with pervasive sericite and neoformed clay minerals; B) advanced stage of biotite alteration replaced by Fe-oxides and abundant clay minerals along rims and lamellae; C) Fe-oxide; D) oxidized and argillaceous matrix; E) early stage of k-feldspar alteration showing fine-grained sericite along the border; F) fractured quartz.

Le Pera, E., Sorriso-Valvo, M., 2000a. Weathering, erosion and sediment composition in a high-gradient river, Calabria, Italy. Earth Surf. Proc. Land. 25, 277–292.

Le Pera, E., Sorriso-Valvo, M., 2000b. Weathering and morphogenesis in a Mediterranean climate, Calabria, Italy. Geomorphology 34, 251–270.

Le Pera, E., Arribas, J., Critelli, S., Tortosa, A., 2001a. The effects of source rocks and chemical weathering on the petrogenesis of siliciclastic sand from the Neto River (Calabria, Italy): implications for provenance studies. Sedimentology 48, 357–378.

Le Pera, E., Critelli, S., Sorriso-Valvo, M., 2001b. Weathering of gneiss in Calabria, Southern Italy. Catena 42, 1–15.

Lee, S.G., De Freitas, D.H., 1989. A revision of the description and classification of weathered granite and its application to granite in Korea. Q. J. Eng. Geol. 22, 31–48.

Lumb, P., 1962. The properties of decomposed granite. Geotechnique 12, 226–243.

Matano, F., Di Nocera, S., 1999. Weathering patterns in the Sila Massif (northern Calabria, Italy). Il Quaternario 12, 141–148.

Messina, A., Barbieri, M., Compagnoni, R., De Vivo, B., Perrone, V., Russo, S., Scott, B.A., 1991. Geological and petrochemical study of the Sila Massif plutonic rocks (Northern Calabria, Italy). Boll. Soc. Geol. Ital. 110, 165–206.

Messina, A., Russo, S., Borghi, A., Colonna, V., Compagnoni, R., Caggianelli, A., Fornelli, A., Piccarreta, G., 1994. Il Massiccio della Sila Settore settentrionale dell'Arco Calabro-Peloritano. Boll. Soc. Geol. Ital. 113, 539–586.

Molin, P., Pazzaglia, F.J., Dramis, F., 2004. Geomorphic expression of active tectonics in a rapidly deforming forearc, Sila Massif, Calabria, southern Italy. Am. J. Sci. 304, 559–589.

Mongelli, G., Cullers, R.L., Dinelli, E., Rottura, A., 1998. Elemental mobility during the weathering of exposed lower crust: the kinzigitic paragneisses from the Serre, Calabria, Southern Italy. Terra Nova 10, 190–195.

Mongelli, G., Critelli, S., Perri, F., Sonnino, M., Perrone, V., 2006. Sedimentary recycling, provenance and paleoweathering from chemistry and mineralogy of Mesozoic continental redbed mudrocks, Peloritani Mountains, Southern Italy. Geochem. J. 40, 197–209.

Moore, D.M., Reynolds, R.C., 1997. X-ray Diffraction and the Identification and Analysis of Clay Minerals: Second Edition. Oxford University Press, Oxford and New York pp. 332.

Olivetti, V., Cyr, A.J., Molin, P., Faccenna, C., Granger, D.E., 2012. Uplift history of the Sila Massif, southern Italy, deciphered from cosmogenic [10]Be erosion rates and river longitudinal profile analysis. Tectonics 31 (TC3007).

Ollier, C., 1983. Weathering or hydrothermal alteration? Catena 10, 57–59.

Ollier, C., 1984. Weathering, Second edition. Longman, London 270.

Ollier, C., 1988. The regolith in Australia. Earth Sci. Rev. 25, 355–361.

Palmentola, G., Acquafredda, P., Fiore, S., 1990. A new correlation of the glacial moraines in the southern Appennines, Italy. Geomorphology 3, 1–8.

Palomares, M., Arribas, J., 1993. Modern stream sands from compound crystalline sources: composition and sand generation index. In: Johnsson, M.J., Basu, A. (Eds.), Processes Controlling the Composition of Clastic Sediments. Geological Society of America, Special Paper, 284, pp. 313–322.

Papoulis, D., Tsolis-Katagas, P., Katagas, C., 2004. Progressive stages in the formation of kaolin minerals of different morphologies in the weathering of plagioclase. Clays Clay Miner. 52, 275–286.

Perri, F., 2008. Clay mineral assemblage of the Middle Triassic–Lower Jurassic mudrocks from Western-Central Mediterranean Alpine Chains. Period. mineral. 77, 23–40.

Perri, F., 2011. SEM observations of silicate minerals affected by weathering processes. In: Zhuang, L., Derek, W. (Eds.), Mica: Properties, Synthesis and Applications. 3. Nova Science Publishers Inc., pp. 59–76.

Perri, F., Cirrincione, R., Critelli, S., Mazzoleni, P., Pappalardo, A., 2008. Clay mineral assemblages and sandstone compositions of the Mesozoic Longobucco Group (north-eastern Calabria): implication for burial history and diagenetic evolution. Int. Geol. Rev. 50, 1116–1131.

Perri, F., Critelli, S., Mongelli, G., Cullers, R.L., 2011a. Sedimentary evolution of the Mesozoic continental redbeds using geochemical and mineralogical tools: the case of Upper Triassic to Lowermost Jurassic Monte di Gioiosa mudrocks (Sicily, southern Italy). Int. J. Earth Sci. 100, 1569–1587.

Perri, F., Muto, F., Belviso, C., 2011b. Links between composition and provenance of Mesozoic siliciclastic sediments from Western Calabria (Southern Italy). Ital. J. Geosci. 130, 318–329.

Perri, F., Borrelli, L., Critelli, S., Gullà, G., 2012. Investigation of weathering rates and processes affecting plutonic and metamorphic rocks in Sila Massif (Calabria, southern Italy). Rend. Online Soc. Geol. Ital. 21, 557–559.

Perri, F., Critelli, S., Martìn-Algarra, A., Martìn-Martìn, M., Perrone, V., Mongelli, G., Zattin, M., 2013. Triassic redbeds in the Malaguide Complex (Betic Cordillera — Spain): petrography, geochemistry, and geodynamic implications. Earth Sci. Rev. 117, 1–28.

Ruxton, P.B., 1958. Weathering and subsurface erosion in granite at the piedmont angle, Balos, Sudan. Geol. Mag. 95, 353–377.

Scarciglia, F., Le Pera, E., Critelli, S., 2005. Weathering and pedogenesis in the Sila Grande Massif (Calabria, South Italy): from field scale to micromorphology. Catena 61, 1–29.

Scarciglia, F., Le Pera, E., Critelli, S., 2007. The onset of the sedimentary cycle in a mid-latitude upland environment: weathering, pedogenesis, and geomorphic processes on plutonic rocks (Sila Massif, Calabria). In: Arribas, J., Critelli, S., Johnsson, M. (Eds.), Sedimentary Provenance and Petrogenesis: Perspectives from Petrography and Geochemistry. Geological Society of America, Special Paper, 420, pp. 149–166.

Sorriso-Valvo, M., Tansi, C., 1996. Grandi frane e deformazioni gravitative profonde di versante della Calabria. Note illustrative della carta al 250.000. Geogr. Fis. Quat. 19, 395–408.

Terranova, O., Antronico, L., Gullà, G., 2007. Landslide triggering scenarios in homogeneous geological contexts: the area surrounding Acri (Calabria, Italy). Geomorphology 87, 250–267.

Thomson, S.N., 1994. Fission-track analysis of the crystalline basement rocks of the Calabrian Arc, southern Italy: evidence of Oligo-Miocene late-orogenic extension and erosion. Tectonophysics 238, 331–352.

Tripodi, V., Muto, F., Critelli, S., 2013. Structural style and tectono-stratigraphic evolution of the Neogene–Quaternary Siderno Basin, southern Calabrian Arc, Italy. Int. Geol. Rev. 4, 468–481.

Velbel, M.A., 1983. A dissolution–reprecipitation mechanism for the pseudomorphous replacement of plagioclase feldspar by clay minerals during weathering. In: Nahon, D., Noack, Y. (Eds.), Petrologie des Alterations et des Sols. Mem. Sc. Geol., 71, pp. 139–147.

Weaver, C.E., 1989. Clays, muds, and shales. Developments in Sedimentology.Elsevier, Amsterdam.

Whalley, W.B., Turkington, A.V., 2001. Weathering and geomorphology. Geomorphology 41, 1–3.

Zaghloul, M.N., Critelli, S., Perri, F., Mongelli, G., Perrone, V., Sonnino, M., Tucker, M., Aiello, M., Ventimiglia, C., 2010. Depositional systems, composition and geochemistry of Triassic rifted-continental margin redbeds of Internal Rif Chain, Morocco. Sedimentology 57, 312–350.